

# Dynamical Response of Fermi Condensate to Varying Magnetic Fields

W. Yi and L.-M. Duan

*FOCUS center and MCTP, Department of Physics, University of Michigan, Ann Arbor, MI 48109*

We investigate the dynamical response of strongly interacting ultra-cold fermionic atoms near Feshbach resonance to varying magnetic fields. Following the experimental practices, we calculate the response of the atoms to oscillating and to linearly ramped magnetic fields respectively. For oscillating magnetic fields, depending on the frequencies and the amplitudes of the oscillations, the response of the pair excitation gap shows either linear or rich non-linear behaviour. In addition, both the spectral studies through the linear response theory and the time-domain simulations suggest the existence of a resonant frequency corresponding to the pair dissociation threshold. For linearly ramped magnetic fields, the response of the excitation gap shows damped oscillations. The final value of the excitation gap depends on the rate of the field sweep.

## I. INTRODUCTION

Feshbach resonance in ultra-cold Fermi gases, where the energy of two scattering atoms is magnetically tuned to coincide with that of a quasi-bound molecular state, has provided a rare opportunity to study strongly correlated many-body systems with tunable interactions [1, 2]. Recently, considerable experimental efforts have been dedicated to the condensation of fermionic atom pairs near Feshbach resonance [3, 4, 5, 6, 7]. The properties of such a Fermi condensate and its crossover to the Bose-Einstein condensation (BEC) of diatomic molecules are currently under active studies [8, 9, 10, 11, 12, 13].

In this paper, we investigate the dynamical response of a Fermi condensate to magnetic field modulations. We study two kinds of modulations, the sinusoidal oscillation and the linear ramp, both of which have been frequently applied in experiments [1, 3, 4, 5, 7, 14, 15]. There have been some recent studies on the atom-molecule oscillations under a sudden switch of the magnetic field [11, 12]. By considering response of the Fermi condensate to more general variations of the magnetic field, we find richer response structures of this strongly interacting system under different driving frequencies or sweep rates. In particular, oscillating magnetic fields have been used recently as important experimental tools to investigate the relaxation time of the Fermi condensate [7]; while fast magnetic field sweeps from the BCS side of Feshbach resonance to the BEC side have been used to probe the properties of the Fermi pairs on the BCS side [3, 4].

In the case of oscillating magnetic fields, we first develop a linear response theory in the frequency domain to describe the dynamics of the Fermi condensate under arbitrary but small variations of the magnetic field. This spectral analysis is then compensated by direct time-domain simulations. The result shows that the response of the Fermi condensate remains linear up to the pair dissociation frequency, around and above which the non-linearity of the system becomes dominant, giving rich non-linear response structure. For linearly ramped magnetic fields, we perform real time evolutions at different ramping rates. The responses of the system are essentially damped atom-molecule oscillations. The final

states of the damping process, however, are dependent on the ramping rates. For adiabatic ramps, the final states are close to the stationary state at the final magnetic field of the field sweep. This is consistent with the experimental practice, where adiabatic sweeps are applied across the Feshbach resonance from the BCS side towards the BEC side to efficiently convert Fermions into Feshbach molecules [14, 15]. In contrast, the final state of a sudden ramp correlates rather with the stationary state at the initial magnetic field.

In the following, we first derive the equations of motion starting from the general two-channel Hamiltonian. Our approach is based on the time-dependent variational theory, by assuming an evolving pair wavefunction as the ansatz state. Then in Sec. III, we apply the equations of motion to study the response of the system to oscillating magnetic fields. We first perform a spectral analysis using the linear response theory to characterize the response spectrum, which is later supported by direct time-domain simulations. In Sec. IV, we apply the equations of motion to study the response of the system to linearly ramped magnetic fields. We conclude with a summary in Sec. V.

## II. MODEL HAMILTONIAN AND THE EQUATIONS OF MOTION

The coupling in strongly interacting Fermi gas near Feshbach resonance can be described by a two-channel model with the Hamiltonian [8, 12, 16, 17, 18, 19]:

$$H = \sum_{\mathbf{k}, \sigma} \varepsilon_{\mathbf{k}} a_{\mathbf{k}, \sigma}^{\dagger} a_{\mathbf{k}, \sigma} + \sum_{\mathbf{k}} (\varepsilon_{\mathbf{k}}/2 + \bar{\gamma}) b_{\mathbf{k}}^{\dagger} b_{\mathbf{k}} + \sum_{\mathbf{k}, \mathbf{q}} \frac{g}{\sqrt{V}} (b_{\mathbf{q}}^{\dagger} a_{\mathbf{k}+\mathbf{q}/2, \uparrow} a_{-\mathbf{k}+\mathbf{q}/2, \downarrow} + h.c.), \quad (1)$$

where  $\varepsilon_{\mathbf{k}} = \hbar^2 \mathbf{k}^2 / 2m$  is the atomic kinetic energy ( $m$  is the mass of the atom),  $g$  is the atom-molecule coupling rate,  $V$  is the volume of the system, and  $a_{\mathbf{k}, \sigma}^{\dagger}$ ,  $b_{\mathbf{k}}^{\dagger}$  are the creation operators for the fermionic atoms and the bosonic bare molecules with momentum  $\hbar \mathbf{k}$ , respectively. Atoms in two different Zeeman levels are labeled

by the spin index  $\sigma$  ( $\sigma = \uparrow, \downarrow$ ). The bare energy detuning  $\bar{\gamma}$  of the quasi-bound molecular level is related to the physical detuning  $\gamma_p = 2\mu_B [B(t) - B_0]$  by the standard renormalization relation  $\bar{\gamma} = \gamma_p + g^2/V \sum_{\mathbf{k}} (1/2\varepsilon_{\mathbf{k}})$  [8, 9, 17]. In the expression for  $\gamma_p$ ,  $B(t)$  is the applied magnetic field which we take to be time-dependent, and  $B_0$  denotes the Feshbach resonance point. In writing this Hamiltonian, we have ignored the background scattering as it is negligible near Feshbach resonance.

The basic method to deal with this system at very low temperature is the crossover theory which is based on the variational assumption that the ground state of the above Hamiltonian can be written as a condensate of the dressed molecules [8, 9, 17, 20]. Here, we extend this variational method to the time-dependent case (with varying  $B(t)$ ) by assuming that the state of the system at any time  $t$  can still be written in the form:

$$|\Phi(t)\rangle = \mathcal{N} \exp[A(t) b_0^\dagger + \sum_{\mathbf{k}} f_{\mathbf{k}}(t) a_{-\mathbf{k},\downarrow}^\dagger a_{\mathbf{k},\uparrow}^\dagger] |vac\rangle, \quad (2)$$

but with time-varying variational parameters  $A(t)$  and  $f_{\mathbf{k}}(t)$  (where  $\mathcal{N}$  is the normalization factor). The parameters  $A(t)$  and  $f_{\mathbf{k}}(t)$  can be identified with  $\langle b_0 \rangle$  and the Cooper-pair wavefunction in  $\mathbf{k}$ -space, respectively. This variational ansatz is reasonable since a condensate state of the form of Eq. (2) is pretty robust against excitations induced by the magnetic field variations: it is unlikely to produce single-atom excitations due to the existence of an energy gap (this is particularly the case when the rate of the field variation is smaller than the energy gap); it is also hard to generate excitations with  $\mathbf{q} \neq 0$  from the  $\mathbf{q} = 0$  condensate due to the momentum conservation.

With the ansatz state above, we minimize the action  $S \equiv \int dt \langle \Phi(t) | (i\partial_t - H) | \Phi(t) \rangle + h.c.$  under  $|\Phi(t)\rangle$ . The functional derivatives of  $S$  with respect to the variational parameters  $A^*(t)$  and  $f_{\mathbf{k}}^*(t)$  give the dynamical evolution equations:

$$i\dot{f}_{\mathbf{k}}(t) = 2\varepsilon_{\mathbf{k}} f_{\mathbf{k}}(t) - \frac{g}{\sqrt{V}} A^*(t) f_{\mathbf{k}}^2(t) + \frac{g}{\sqrt{V}} A(t), \quad (3)$$

$$i\dot{A}(t) = \frac{g}{\sqrt{V}} \sum_{\mathbf{k}} \frac{f_{\mathbf{k}}(t)}{1 + |f_{\mathbf{k}}^2(t)|} + \bar{\gamma} A(t). \quad (4)$$

The above evolution equations can be arranged into a more convenient form if one introduces the pseudo-spin operators  $\sigma_{\mathbf{k}}^- = a_{\mathbf{k},\uparrow} a_{-\mathbf{k},\downarrow}$ ,  $\sigma_{\mathbf{k}}^+ = a_{-\mathbf{k},\downarrow}^\dagger a_{\mathbf{k},\uparrow}^\dagger$ ,  $\sigma_{\mathbf{k}}^z = n_{\mathbf{k},\uparrow} + n_{-\mathbf{k},\downarrow} - 1$  (where  $n_{\mathbf{k},\uparrow} = a_{\mathbf{k},\uparrow}^\dagger a_{\mathbf{k},\uparrow}$ ) [12, 17, 21]. Under the variational state (2), it is easy to check that the mean values of these pseudo-spin operators are uniquely related to the pair-wavefunction  $f_{\mathbf{k}}(t)$  through  $f_{\mathbf{k}} = (\langle \sigma_{\mathbf{k}}^z \rangle + 1) / (2 \langle \sigma_{\mathbf{k}}^+ \rangle)$  and the natural constraint  $4 \langle \sigma_{\mathbf{k}}^+ \rangle \langle \sigma_{\mathbf{k}}^- \rangle + \langle \sigma_{\mathbf{k}}^z \rangle^2 = 1$ . With these relations, the evolution equations (3-4) can be written in terms of the expectation values of the pseudo-spin operators:

$$i\dot{\langle \sigma_{\mathbf{k}}^- \rangle} = 2\varepsilon_{\mathbf{k}} \langle \sigma_{\mathbf{k}} \rangle - \Delta \langle \sigma_{\mathbf{k}}^z \rangle, \quad (5)$$

$$i\dot{\langle \sigma_{\mathbf{k}}^z \rangle} = 2\Delta \langle \sigma_{\mathbf{k}}^- \rangle^* - 2\Delta^* \langle \sigma_{\mathbf{k}}^- \rangle, \quad (6)$$

$$i\dot{\Delta} = \frac{g^2}{V} \sum_{\mathbf{k}} \langle \sigma_{\mathbf{k}}^- \rangle + \bar{\gamma} \Delta, \quad (7)$$

where the parameter  $\Delta \equiv g \langle b_0 \rangle = gA(t)$  is physically identified as the excitation gap for fermionic excitations [20]. The set of equations (5-7) can also be derived by replacing the operators with their mean values in the Heisenberg evolution equations for  $\sigma_{\mathbf{k}}^-, \sigma_{\mathbf{k}}^z$ , and  $b_0$  [12, 17]. The derivation here provides a different physical interpretation of the basic approximation: it is equivalent to an extension of the variational ansatz for the crossover theory [8, 9, 17, 20] to the time-dependent case.

To investigate how the system responds to the variations of the magnetic field (which varies the detuning  $\bar{\gamma}$ ), we look at the evolution of a detectable property, which we choose as the gap function  $\Delta(t)$ . The gap  $\Delta(t)$  is proportional to the occupation in the bare molecular level, and is directly measurable, for instance, through the radio-frequency spectroscopy [22, 23] or the bare molecule population detection [24]. In the subsequent sections, we will examine the response of the system to magnetic field oscillations and linear sweeps at different rates, respectively.

### III. RESPONSE TO OSCILLATIONS OF THE MAGNETIC FIELD

To characterize the response of the system to arbitrary, yet small, magnetic field oscillations, we expand  $\Delta(t)$ ,  $\langle \sigma_{\mathbf{k}}^- \rangle(t)$ ,  $\langle \sigma_{\mathbf{k}}^z \rangle(t)$  around their stationary values, and linearize the resultant evolution equations. The stationary values are obtained from the conventional crossover theory: we minimize  $\langle H - \mu N \rangle$  with a fixed initial detuning  $\gamma_p = \gamma_0$ , and get the following gap and number equations characterizing the stationary state [8]:

$$(\gamma_0 - 2\mu) = \frac{g^2}{V} \left( \sum_{\mathbf{k}} \frac{1}{2E_{\mathbf{k}}} - \frac{1}{2\varepsilon_{\mathbf{k}}} \right), \quad (8)$$

$$n = 2 \frac{\Delta_0^2}{g^2} + \sum_{\mathbf{k}} \left( 1 - \frac{\varepsilon_{\mathbf{k}} - \mu}{E_{\mathbf{k}}} \right), \quad (9)$$

where  $N = \sum_{\mathbf{k},\sigma} a_{\mathbf{k},\sigma}^\dagger a_{\mathbf{k},\sigma} + 2 \sum_{\mathbf{k}} b_{\mathbf{k}}^\dagger b_{\mathbf{k}}$  denotes the total atom number,  $\mu$  is the Lagrange multiplier with the meaning of atomic chemical potential, and  $E_{\mathbf{k}} = \sqrt{(\varepsilon_{\mathbf{k}} - \mu)^2 + \Delta_0^2}$  denotes the single-atom excitation spectrum in the stationary case. From the stationary equations, the gap  $\Delta_0$  and the chemical potential  $\mu$  in the stationary state can be solved, from which the stationary values of the pseudospins are obtained as follows:

$$\langle \sigma_{\mathbf{k}}^- \rangle = -\frac{\Delta_0}{2E_{\mathbf{k}}} \quad (10)$$

$$\langle \sigma_{\mathbf{k}}^z \rangle = -\frac{\varepsilon_{\mathbf{k}} - \mu}{E_{\mathbf{k}}}. \quad (11)$$

From the linearized evolution equations, we can find out the response relation between  $\delta\Delta(t) \equiv \Delta(t) -$

$\Delta_0 e^{-2i\mu t}$  and  $\delta\gamma(t) \equiv \gamma_p - \gamma_0 = 2\mu_B [B(t) - B(0)]$ , where  $B(0)$  is the initial magnetic field. It is convenient to express this response relation in terms of their Fourier transforms  $\delta\Delta(\omega) \equiv \int \delta\Delta(t) e^{-i(\omega-2\mu)t} dt$  and

$\delta\gamma(\omega) \equiv \int \delta\gamma(t) e^{-i\omega t} dt$ . The general response relation can then be written as  $\delta\Delta(\omega) = P(\omega) \delta\gamma(\omega)$ , with the response function  $P(\omega)$  given by:

$$P(\omega) = \frac{\Delta_0 (F(\omega) - G^*(-\omega) + \omega - (\gamma_0 - 2\mu))}{(\omega + G(\omega) + (\gamma_0 - 2\mu))(-\omega + G^*(-\omega) + (\gamma_0 - 2\mu)) - F(\omega)F^*(-\omega)}, \quad (12)$$

in which

$$F(\omega) = \frac{g^2}{2\pi^2 E_F} \int k^2 dk \frac{\Delta_0^2}{4E_k(E_k^2 - \frac{\omega^2}{4})}, \quad G(\omega) = \frac{g^2}{2\pi^2 E_F} \int k^2 dk \left( \frac{-E_k^2 - (\varepsilon_k - \mu)^2 + (\varepsilon_k - \mu)\omega}{4E_k(E_k^2 - \frac{\omega^2}{4})} + \frac{1}{2\varepsilon_k} \right).$$

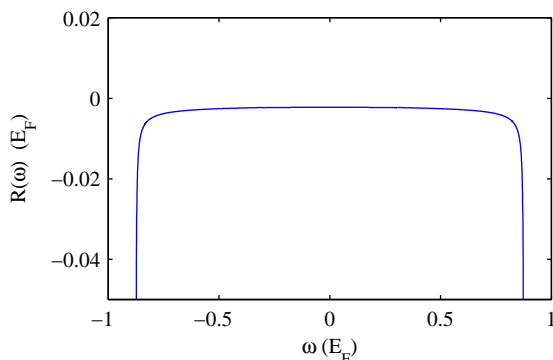


FIG. 1: (Color online) The response function shown in the range  $|\omega| < 2\Delta_0$  (here,  $2\Delta_0 \sim 0.87E_F$ , and  $\omega$  is in the unit of  $E_F$ ). Other parameters are comparable with the  $^{40}\text{K}$  experiments [3], where  $g\sqrt{n} \sim 13.8E_F$  ( $n$  is the atom number density and  $\gamma_0 \sim 100E_F$ ).

The response function  $P(\omega)$  specified by the above equations can not be directly compared with the experimental measurements as it is  $|\Delta|$  that is measured. It is easy, however, to construct the response function  $R(\omega)$  for  $\delta|\Delta| \equiv |\Delta| - \Delta_0$  from  $P(\omega)$  with the following simple connection:

$$R(\omega) = \frac{1}{2}[P(\omega) + P^*(-\omega)]. \quad (13)$$

The resultant spectrum for  $R(\omega)$  is numerically calculated and shown in Fig. 1, with  $\omega$  in the range  $-2\Delta_0 < \omega < 2\Delta_0$  [25], and other parameters comparable with the  $^{40}\text{K}$  experiments [3]. The spectrum shows that the response of the Fermi condensate is linear for small driving fields with the response function only weakly dependent on the driving frequency. The spectrum also shows resonance behaviour at  $\omega = 2\Delta_0$ , which can be associated with the pair dissociation frequency.

To complement the above linear response calculations, we also simulate the evolutions of the gap function  $\Delta(t)$  from Eqs. (5-7) directly in the time domain, with si-

nusoidal magnetic fields at different driving frequencies. With this temporal simulation, we would like to first confirm the resonance predicted by the linear response theory and second find out the validity region for the linear response theory and reveal some non-linear behaviours. In the simulation, we start from an equilibrium state at the positive detuning ( $B(0) > B_0$ ), and assume that the variation of the detuning takes the form  $\delta\gamma(t) = \gamma_p - \gamma_0 = \gamma_{amp} \sin(\omega t)$ , with  $\gamma_0 = 100E_F$  (corresponding to  $(B(0) - B_0) \sim 0.2G$  for  $^{40}\text{K}$ ) and a small oscillation amplitude  $\gamma_{amp} = 1E_F$  ( $E_F = (3\pi^2\hbar^3 n)^{2/3}/2m$  is the Fermi energy, where  $n$  is the atom number density and  $m$  is the mass of the atom). The results of the evolutions are shown in Fig. 2 with several characteristic driving frequencies. For driving frequencies much smaller than  $2\Delta_0$  (Fig. 2a), the  $\delta|\Delta(t)|$  follows the same sinusoidal curve as  $(B(0) - B(t))$  with almost no detectable delay. This shows that the system responds very fast to the changes of the magnetic field, with a time scale much shorter than the thermal relaxation time reported in the recent experiment [7, 26]. When the driving frequency approaches  $2\Delta_0$  (Fig. 2b), some non-linearities show up in the response with a periodic modulation of the oscillation amplitude. For  $\omega = 2\Delta_0$  (Fig. 2c), the resonance behaviour is apparent. The amplitude of the oscillation continuously increases within the time interval attainable in the simulation. For the driving frequency significantly larger than  $2\Delta_0$  (Fig. 2d), the response is almost linear at the beginning, then the nonlinearity shows up causing increase of the oscillation amplitude. We have also simulated the time evolution of the gap function  $\Delta(t)$  with a much larger oscillation amplitude of the driving field corresponding to  $\gamma_{amp} = 50E_F$ . For small non-resonant driving frequencies, the response is still linear even with such a large driving amplitude. For instance, with the same  $\omega$  as in Fig. 2a but  $\gamma_{amp} = 50E_F$ , the response curve of  $\delta|\Delta(t)|$  still has the same shape, although its amplitude is amplified by a factor of 50 as one expects from the linear response theory. For driving frequencies larger than  $2|\Delta_0|$ , even if they are non-resonant, rich

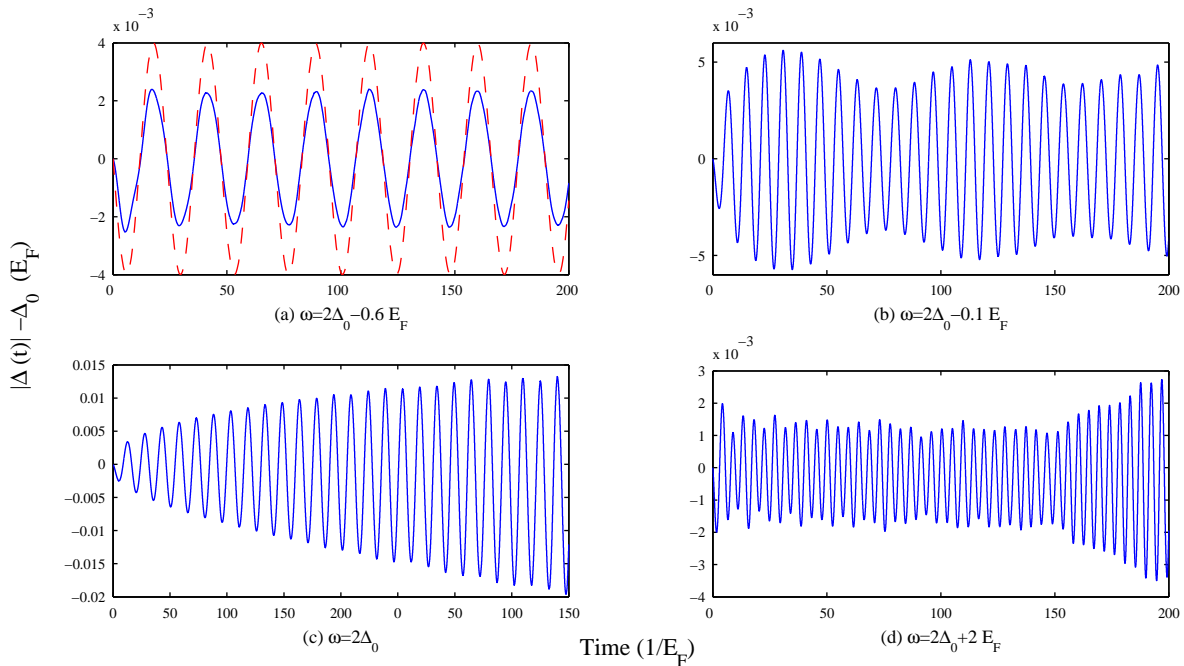


FIG. 2: (Color online) The real-time (in the unit of  $1/E_F, \sim 120\mu s$  for  $^{40}K$  experiments [3]) evolutions of the pair excitation gap  $|\Delta(t)|$  (in the unit of  $E_F$ ) shifted by the initial gap  $\Delta_0$  ( $\Delta_0 \sim 0.433E_F$ ). The system is driven by sinusoidally oscillating magnetic fields at different driving frequencies  $\omega$ . The solid lines represent the evolutions of the excitation gap  $\delta|\Delta(t)|$ , while the dashed line is the re-scaled magnetic field variation  $B(0) - B(t)$ . In all cases,  $\gamma_{amp} = 1E_F$ ,  $g\sqrt{n} \sim 13.8E_F$ , and  $\gamma_0 = 100E_F$ .

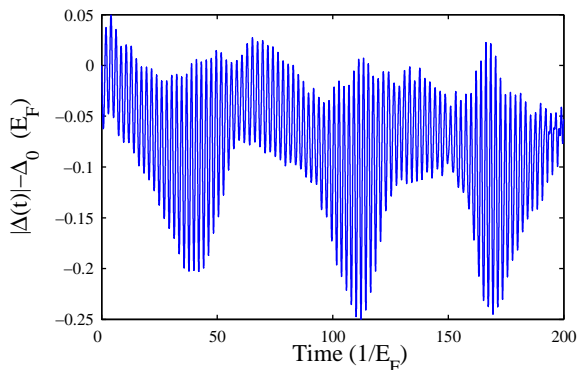


FIG. 3: (Color online) The real-time evolution of the pair excitation gap  $|\Delta(t)|$  shifted by the initial gap  $\Delta_0$ . The same parameters as in Fig. 3d but with a larger driving amplitude  $\gamma_{amp} = 50E_F$ , which roughly corresponds to  $0.15G$  in the  $^{40}K$  experiments [3].

non-linear structure shows up in the response, as one can see in Fig. 3.

#### IV. RESPONSE TO LINEARLY RAMPED MAGNETIC FIELDS

Another branch of important experimental practice is to probe the properties of the Fermi condensate by ramp-

ing the magnetic field from the BCS side of the Feshbach resonance to the BEC side. Slow adiabatic ramps are used to create molecular condensates [14, 15], while fast sudden ramps are used to project the correlated pairs onto Feshbach molecules so as to probe the properties of the Fermi condensate on the BCS side of the resonance [3, 4]. It is desirable then, to understand the ramping process and the effects of the ramping rate. In this section, we study the response of the system to linearly ramped magnetic fields with different ramping rates.

Similar to the previous section, where we vary the magnetic field by modulating the detuning in Eq. (7), now we impose a detuning in the form  $\gamma_p = \gamma_0 - (\gamma_0 - \gamma_f)t/T_{ramp}$ , where  $\gamma_0, \gamma_f$  are the initial and final detunings respectively, and  $T_{ramp}$  is the duration of the field sweep. To facilitate comparison between processes with different ramping rates, once the detuning has been ramped to  $\gamma_f$ , the final detuning, we let the system evolve under this constant magnetic field. Again, we use the pair excitation gap  $\Delta(t)$  to represent the response of the Fermi condensate. As the numerical simulation is quite time consuming at large coupling rates, for the sake of efficiency, we set the atom-molecule coupling rate to be  $g\sqrt{n} \sim 10E_F$ , which is slightly smaller than that of the  $^{40}K$  system, where  $g\sqrt{n} \sim 13.8E_F$ [3]. Qualitatively, the results should not be affected by this change of coupling rate. We perform real-time evolutions of the excitation gap based on Eqs. (5-7), and the results are shown in Fig. 4. The most prominent feature of the results is

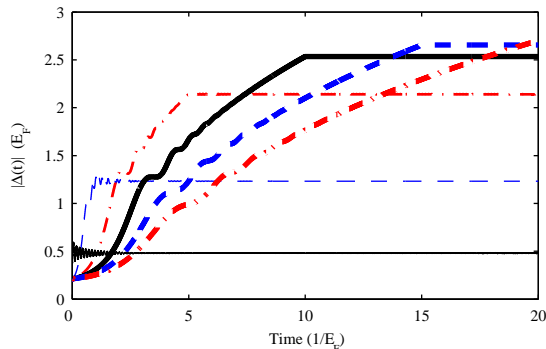


FIG. 4: (Color online) The real-time evolutions of the pair excitation gap  $|\Delta(t)|$  under linear magnetic field sweeps with different sweep rates. While the thin solid curve represents the evolution under a sudden ramp, the ramping time  $T_{ramp}$ , as defined in the text, for the rest of the curves are:  $T_{ramp} = 1/E_F$  for the thin dashed curve,  $T_{ramp} = 5/E_F$  for the thin dash-dot curve,  $T_{ramp} = 10/E_F$  for the thick solid curve,  $T_{ramp} = 15/E_F$  for the thick dashed curve, and  $T_{ramp} = 20/E_F$  for the thick dash-dot curve. The atom-molecule coupling rate is taken to be  $g\sqrt{n} \sim 10E_F$ , with the initial detuning  $\gamma_0 = 100E_F$ , and the final detuning  $\gamma_f = -500E_F$ .

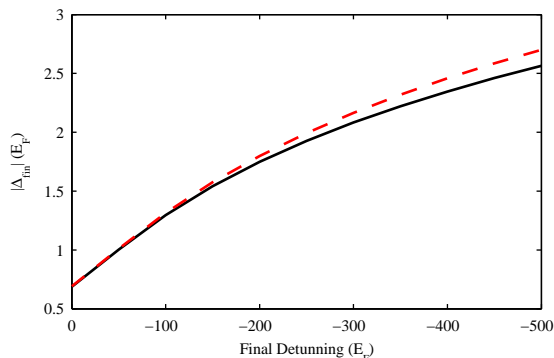


FIG. 5: (Color online) Comparison between the final excitation gap values resulting from slow ramps ( $T_{ramp} = 20/E_F$ ) to different final detunings, with those of the stationary states at the corresponding final detunings. The solid line represents the stationary gap values, and the dashed line represents the final gap values of the slow ramps. The starting points of all the field ramps are fixed at  $\gamma_0 = 100E_F$ , while the final detunings are varied over the range of  $\gamma_f = 0 \sim -500E_F$ . The atom-molecule coupling is taken to be  $g\sqrt{n} \sim 10E_F$ .

that the excitation gap undergoes damped oscillations under fast field sweeps. This result is in agreement with Ref. [11] for the particular case of a sudden sweep, but is in contrast to the undamped oscillations reported in [12]. We expect that this kind of damped oscillations is a general response behaviour for a system with many degrees of freedom as is the case here; the undamped oscillations on the other hand should be a more artificial effect resulting from some unrealistic constraints. For

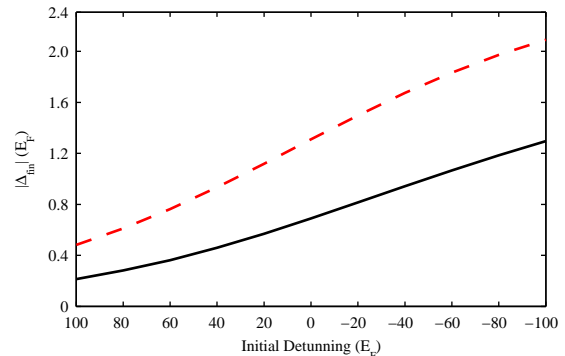


FIG. 6: (Color online) Comparison between the the final excitation gap values resulting from sudden ramps from different initial detunings, with those in the stationary states at the corresponding initial detunings. The solid line represents the stationary gap values, and the dashed line corresponds to the final gap values of the sudden ramps. The final detunings of all the field ramps are fixed at  $\gamma_f = -500E_F$ , while the initial detunings are varied over the range of  $\gamma_0 = 100E_F \sim -100E_F$ . The atom-molecule coupling is taken to be  $g\sqrt{n} \sim 10E_F$ .

slower sweeps, the damping also occurs along with the sweep but with a relatively smaller amplitude; and if the sweep rate is slow enough, the absolute value of the excitation gap will follow the field sweep almost adiabatically. Another important feature is that the final state of the system, reflected in the absolute value of the final gap, depends on the rate of the field sweep. Even though the initial and the final detunings are set to be the same in all the evolutions in Fig. 4, there appear to be considerable differences in the values of the final gap at different ramping rates. These rate-dependent “stationary states” are different from the stationary states calculated in Sec. III with Eqs. (8-9). The final state at a given ramping rate is one such that the absolute value of the excitation gap is not evolving but its phase changes with time. Even under such a final “stationary” state with a constant  $|\Delta(t)|$ , numerical analysis shows that there still appear to be complicated momentum-dependent oscillations of the pseudospins  $\langle\sigma_{\mathbf{k}}^+\rangle$ ,  $\langle\sigma_{\mathbf{k}}^-\rangle$ , and  $\langle\sigma_{\mathbf{k}}^z\rangle$ , which effectively describe the shape oscillations of the dressed molecules. The amplitude of such oscillations decreases as the sweep rate approaches the adiabatic limit, and in the adiabatic limit, the state just follows the real stationary state of the system determined by Eqs. (8-9) as the detuning decreases.

Among these many ramping-rate dependent final states, of particular interest to us are the final state of a sudden ramp and the final state of an adiabatic ramp, due to their close experimental relevance. To study the property of the final states, we compare the excitation gap in the stationary state at either the initial or the final detuning with the gap in the final state of the evolution. One can either fix the initial detuning while changing the final detuning of the field sweep or the other way around.

We have plotted in Fig. 5 and Fig. 6. the results of our simulations. For a very slow ramp, if one fixes the initial detuning and varies the final detuning, the final gap would approach the stationary values of the gap at those different  $\gamma_f$ . The differences between the two curves in Fig. 5 can be made smaller by decreasing the ramping rate further. This is in agreement with the experiment [14], where slow field sweeps, which roughly correspond to ramp time of over  $100/E_F$  to cover the same detuning range in Fig. 4, were applied to create molecules. In a sudden ramp, one needs to fix the final detuning while varying the initial starting point. It appears, as in Fig. 6, that there exist correlations between the final gap and the initial gap, while both are much smaller than the stationary value of the gap at the final detuning. There are no such correlations if one fixes the initial detuning and vary the final detuning. This result is in agreement with Ref. [11] from a single channel calculation. The finding also agrees with the experimental practice that a fast projection would allow us to probe information in the initial state.

## V. SUMMARY

In summary, we have investigated the dynamical response of a Fermi condensate near Feshbach resonance to external magnetic field modulations. For a sinusoidal modulation with small amplitude and frequency, the response of the Fermi condensate linearly follows the mod-

ulation. The linear behaviour breaks down when the frequency of the modulated field approaches the pair dissociation frequency  $2\Delta_0$ . The response of the system will be composed of highly non-linear structures if the frequency increases above this threshold. Calculations of the response spectrum using the linear response theory as well as real time evolutions consistently support the conclusions. We have also calculated the real time evolutions of the pair excitation gap under linearly ramped magnetic fields, the results of which are consistent with the experimental observations. The general feature of the response to the field sweep is the damped oscillations, which are more manifest in faster sweeps. The final state of the sweep depends on the rate of the sweep. While the final state of a slow ramp is quite close to the stationary state at the final detuning; that of a sudden ramp correlates with the stationary state at the initial detuning, as can be seen from the correlations between the final gap and the initial gap in a sudden ramp. The results are in agreement with the experimental practices that adiabatically slow field sweeps efficiently convert Fermion pairs on the BCS side of the Feshbach resonance into bound molecules deep in the BEC side; and that sudden field sweeps project the Fermion pairs onto the molecules, so that the properties of the initial state can be probed via measurements of the final state.

This work was supported by the NSF awards (0431476), the ARDA under ARO contracts, and the A. P. Sloan Fellowship.

- 
- [1] S. Inouye *et al.*, Nature **392**, 151 (1998)
  - [2] R.A. Duine and H.T.C. Stoof, Phys. Rep. **396**, 115 (2004).
  - [3] C.A. Regal, M. Greiner and D.S. Jin, Phys. Rev. Lett. **92**, 040403 (2004).
  - [4] M.W. Zwierlein *et al.*, Phys. Rev. Lett. **92**, 120403 (2004).
  - [5] M. Bartenstein *et al.*, Phys. Rev. Lett. **92**, 120401 (2004).
  - [6] J. Kinast *et al.*, Phys. Rev. Lett. **92**, 090402 (2004).
  - [7] M.W. Zwierlein *et al.*, Phys. Rev. Lett. **94**, 180401 (2005).
  - [8] R.B. Diener and T.L. Ho, arXiv.condmat/0405174, (2004).
  - [9] G.M. Falco and H.T.C. Stoof, Phys. Rev. Lett. **92**, 130401 (2004).
  - [10] M. Haque and H.T.C. Stoof, Phys. Rev. A **71**, 063603 (2005).
  - [11] M.H. Szymanska, B.D. Simons and K. Burnett, Phys. Rev. Lett. **94**, 170402 (2005).
  - [12] R.A. Barankov and L.S. Levitov, Phys. Rev. Lett. **93**, 130403 (2004).
  - [13] E. Altman and A. Vishwanath, arXiv.condmat/0501683, (2005).
  - [14] M. Greiner, C.A. Regal, and D.S. Jin, Nature **426**, 537 (2003).
  - [15] M.W. Zwierlein *et al.*, Phys. Rev. Lett. **91**, 250401 (2003).
  - [16] Q.J. Chen *et al.*, Phys. Rep. **412**, 1 (2005).
  - [17] A.V. Andreev, V. Gurarie and L. Radzihovsky, Phys. Rev. Lett., **93**, 130402 (2004).
  - [18] M. Holland *et al.*, Phys. Rev. Lett. **87**, 120406 (2001).
  - [19] Y. Ohashi and A. Griffin, Phys. Rev. Lett. **89**, 130402 (2002).
  - [20] A.J. Leggett, J. Phys. C. (Paris) **41**, 7 (1980).
  - [21] P.W. Anderson, Phys. Rev. **112**, 1900 (1958).
  - [22] P. Törmä and P. Zoller, Phys. Rev. Lett. **85**, 487 (2000).
  - [23] C. Chin *et al.*, Science **305**, 1128 (2004).
  - [24] G. B. Partridge *et al.*, Phys. Rev. Lett. **95**, 020404 (2005).
  - [25] As discussed before, the variational ansatz (2) should be a good approximation for  $\omega$  in the range  $|\omega| < 2\Delta_0$ .
  - [26] When the condensed dressed molecules (with  $\mathbf{q} = 0$ ) and the thermal cloud (with  $\mathbf{q} \neq 0$ ) are pushed into a non-equilibrium state, the thermal relaxation time, which characterizes the time scale for them to re-obtain the thermal equilibrium, is long compared with  $1/E_F$ .